



# A simple approach for reconstruction of non-uniformly sampled pseudo-3D NMR data for accurate measurement of spin relaxation parameters

Kyle W. East<sup>1</sup> · Frank Delaglio<sup>2</sup> · George P. Lisi<sup>1</sup>

Received: 17 February 2021 / Accepted: 4 May 2021 / Published online: 7 May 2021  
© The Author(s), under exclusive licence to Springer Nature B.V. 2021

## Abstract

We explain how to conduct a pseudo-3D relaxation series NUS measurement so that it can be reconstructed by existing 3D NUS reconstruction methods to give accurate relaxation values. We demonstrate using reconstruction algorithms IST and SMILE that this 3D approach allows lower sampling densities than for independent 2D reconstructions. This is in keeping with the common finding that higher dimensionality increases signal sparsity, enabling lower sampling density. The approach treats the relaxation series as ordinary 3D time-domain data whose imaginary part in the pseudo-dimension is zero, and applies any suitably linear 3D NUS reconstruction method accordingly. Best results on measured and simulated data were achieved using acquisitions with 9 to 12 planes and exponential spacing in the pseudo-dimension out to ~2 times the inverse decay time. Given these criteria, in typical cases where 2D reconstructions require 50% sampling, the new 3D approach generates spectra reliably at sampling densities of 25%.

**Keywords** Non-uniform sampling · Spin relaxation · Spectral reconstruction

## Abbreviations

1D	One-dimensional
2D	Two-dimensional
3D	Three-dimensional
DFT	Discrete Fourier transform
FID	Free induction decay
IST	Iterative soft thresholding reconstruction
nD	Multidimensional
NMR	Nuclear magnetic resonance spectroscopy
NUS	Non-uniformly sampled
RF	Radio frequency
SMILE	Sparse multidimensional iterative line shape enhanced reconstruction

Non-uniform sampling (NUS) methods can provide better spectral quality with less measurement time (Hyberts et al. 2014; Mobli and Hoch 2014; Robson et al. 2019). NUS reduces experiment time by collecting only a fraction of the total data within the uniform grid of time domain points in the indirect dimensions, necessitating the use of non-Fourier methods to reconstruct spectra. Several sampling strategies have been explored, including sampling densities that are uniform-random, exponentially weighted, or Poisson-gap weighted according to sine and cosine distributions (Barna et al. 1987; Schmieder et al. 1994; Hyberts et al. 2010; Hyberts et al. 2012). Likewise, many NUS reconstruction algorithms have been demonstrated, including MDD (Orekhov and Jaravine 2011), IST (Stern et al. 2007; Hyberts et al. 2012), SMILE (Ying et al. 2017), and others (Bostock and Nietlispach 2017; Hansen 2019), and the effects of the sampling schedule on artifacts in reconstructed spectra have been well characterized (Hoch et al. 2008; Worley and Powers 2015). Due to the ease of implementing NUS on modern NMR spectrometers, and the prevalence of robust reconstruction methods, NUS has become a prominent method for rapid collection of complex NMR spectra, and is widely utilized in 2D, 3D and nD experiments for biomolecular NMR where resolution of signals is critical. However, NUS is not widely used in experiments probing protein dynamics

✉ George P. Lisi  
george\_lisi@brown.edu

<sup>1</sup> Department of Molecular Biology, Cell Biology, and Biochemistry, Brown University, Providence, RI 02903, USA

<sup>2</sup> Institute of Bioscience and Biotechnology Research, National Institute of Standards and Technology, The University of Maryland, 9600 Gudelsky Dr. Rockville, College Park, MD 20850, USA

(i.e. relaxation). This can be attributed to the importance of the relative signal intensity in relaxation parameter fitting, which is a potential challenge since NUS reconstruction methods are generally non-linear, and therefore could change relative intensities. Early NUS reconstruction techniques emphasized frequency resolution, but spin relaxation experiments that rely heavily on quantitation of relative signal intensities across a series of spectra (Loria et al. 1999; Kleckner and Foster 2011) have not benefited as widely from NUS despite the emergence of better reconstruction methods (Linnet and Teilum 2016; Urbanczyk et al. 2017). Given the ever-increasing body of work suggesting that protein dynamics spanning the full breadth of NMR-detectable timescales are necessary for understanding protein function (Lisi and Loria 2016; Maria-Solano et al. 2018) and pharmacodynamics (Amaral et al. 2017), it is useful to optimize NUS methods that provide access to faithful dynamic information within a practical time frame.

Two of the most widely utilized spin relaxation experiments,  $T_1$  and  $T_2$ , are collected as a set of 2D frequency domain spectra, where each 2D spectrum is measured with a set  $T_1$  or  $T_2$  delay,  $\tau$ , as reviewed in (Palmer 2004). Therefore, these experiments can be collectively considered a pseudo-three-dimensional (pseudo-3D) experiment where the directly detected dimension ( $^1\text{H}$ ) and indirectly detected dimension ( $^{15}\text{N}$ ) can be processed by Fourier transform. The pseudo-3<sup>rd</sup> dimension is the dynamic dimension, which remains unprocessed as time domain data with each 2D plane corresponding to a value of  $\tau$ . The relative intensity of each signal in the final processed spectral series is fit to an exponential decay to extract the relaxation time:

$$\frac{I(\tau)}{I_0} = e^{-\frac{\tau}{\alpha}} \quad (1)$$

where  $I(\tau)$  is the relative intensity with a relaxation delay of time  $\tau$  in seconds,  $I_0$  is the initial intensity, and  $\alpha$  is the characteristic decay time of the signal ( $T_1$  or  $T_2$ ) in seconds. The common practice for these series measurements is to use  $\tau$  values in random order to redistribute systematic errors due to temperature fluctuation and sample stability.

This methodology has become ubiquitous for extracting dynamic information from biomolecules by NMR. However, in order to obtain accurate and precise relaxation parameters, the resonance intensity for every 2D plane of the pseudo-3D dataset must be faithfully reconstructed, which can be challenging when non-Fourier methods are used (Schmieder et al. 1997). Pseudo-3D NUS relaxation data have been effectively treated by methods such as Matrix Decomposition, at the expense of including a fully sampled initial dataset and ~16 planes (Kazimierczuk and Orekhov 2011; Orekhov and Jaravine 2011; Qu, Mayzel et al. 2015; Linnet and Teilum 2016).

In this work, we introduce a simple approach for NUS reconstruction of pseudo-3D datasets (pseudo-NUS) that can use existing NUS algorithms to reconstruct spectra with accurate relative intensities in each plane. This method is currently implemented in NMRPipe (Delaglio et al. 1995). While we implemented this protocol using IST and SMILE algorithms, this methodology can in principle be extended to other NUS reconstruction methods. As with the existing 2D–4D NUS reconstruction tools in NMRPipe, the new reconstruction method can be performed by a single command (Fig. S1), or via a graphical interface (Fig. S2), and processing of all conventional and NUS spectra in the current work required specification of only phase correction options and region of interest limits.

In their successful approach to apply matrix decomposition to pseudo-3D data, Kazimierczuk and Orekhov note that experiments such as relaxation series have a similar mathematic form to conventional 3D data, allowing them to be treated by the same matrix decomposition approaches. Our new method is similarly straightforward: the pseudo-dimension is simply treated as an additional time-domain dimension whose imaginary part is zero, and as if the time increment between points is uniform. Conventional 3D NUS reconstruction is employed to generate a 3D spectrum, and then the pseudo-dimension is inverse transformed to generate the interpolated pseudo-3D result (Fig. S1). Here, we show that this method can be used to reconstruct sparsely sampled  $T_1$  and  $T_2$  data and that these reconstructed spectra can be used to extract accurate relaxation parameters.

While the effects of relaxation measurement parameters have been well characterized (Baselice et al. 2014), we characterized these details in the context of this new method. To test the ability of pseudo-NUS to reconstruct pseudo-3D data with accurate relative intensities, fully sampled  $T_1$  and  $T_2$  datasets were collected on the HNH domain from *S. pyogenes* CRISPR-Cas9 (East et al. 2020) using a standard set of 10 total relaxation delays containing three repeated  $\tau$  values, with 1024 complex points in the  $^1\text{H}$  dimension and 128 complex points in the  $^{15}\text{N}$  dimension. An additional fully sampled  $T_2$  dataset was collected using a set of 12 delays and no duplicate  $\tau$  values, and with the last four planes out of  $\tau$  order. The 2D planes of these spectra contain about 130 peaks, with noise levels ~0.2% of the largest signals. Acquisition and processing details are given in Fig. S1.

Figure 1 compares spectra from fully sampled data and the same data resampled at 25% uniform random density, as reconstructed by the new 3D pseudo-NUS method (Fig. 1a) and with conventional 2D NUS reconstruction of each plane (Fig. 1b). As shown, the 3D pseudo-NUS reconstruction looks almost identical to the uniformly sampled spectrum, while the conventional 2D NUS reconstruction shows substantial artifacts at this sampling density. In a point-by-point comparison of spectral intensities (Fig. 1c), the Pearson's

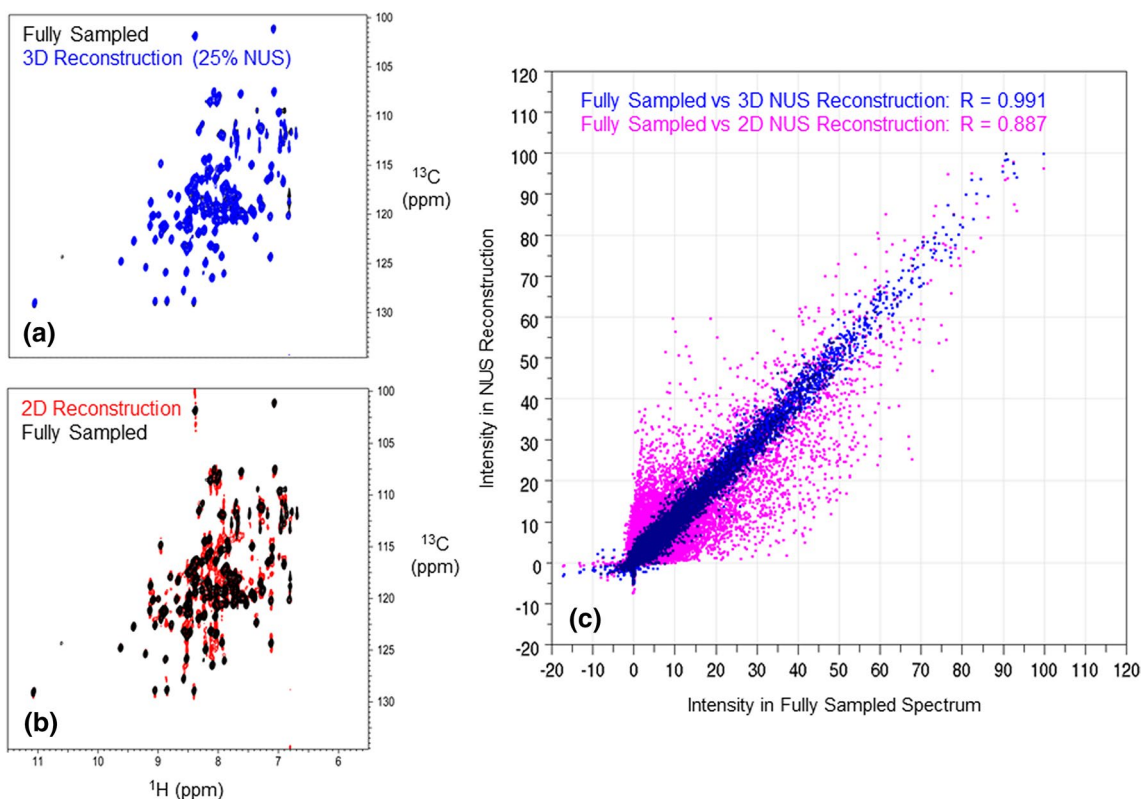


**Fig. 1** Comparison of conventional plane-wise 2D NUS reconstruction of a 12-plane  $T_2$  series to the new 3D pseudo-NUS reconstruction method. **a** Overlay of the first plane of the  $T_2$  series comparing the fully sampled spectrum (black) and the 25% NUS spectrum reconstructed with the new 3D method (blue). **b** Overlay of the first plane of the  $T_2$  series comparing 25% NUS 2D-reconstructed spec-

trum (red) to the fully sampled spectrum (black). **c** Correlation of intensities of each point in the normalized plane of the 2D IST reconstruction (pink, Pearson's correlation coefficient  $R$  0.887) and pseudo-3D IST reconstruction (blue, Pearson's  $R$  0.991) to the intensities of the same point in the fully sampled spectrum. Acquisition and processing details are given in the supplemental information

correlation coefficient between the fully sampled data and the 2D IST result was 0.887, while the correlation to the 3D result was 0.991. The 3D pseudo-NUS approach provides a substantial improvement in the quality of each reconstructed plane when compared to a standard IST reconstruction of each individual 2D plane, and importantly, the relative intensities of the reconstructed spectrum are closer to the Fourier transformed, fully sampled spectrum.

In order for a NUS reconstruction to be successful, the signals in the spectrum must be “sparse” (roughly, more empty space than signal), the measurement must have a sufficient number of samples to account for the number of signals in the data, and the sampling schedule should be incoherent. (Monajemi and Donoho 2019; Nichols et al. 2020). It is commonly observed that increasing dimensionality increases signal sparsity, so that an additional dimension of even a small number of points can be beneficial for NUS (Bostock et al. 2012). For a spectral series with  $N$  peaks in a plane and  $M$  total planes, the new method replaces the task of reconstructing  $N \times M$  2D signals with the easier task of reconstructing  $N$  3D signals. The 3D approach has the

additional benefit that the pseudo-dimension can introduce an additional source of incoherence, improving NUS reconstruction (Schuyler et al. 2015). As a consequence of signal sparsity, the 3D pseudo-NUS method is expected to be more effective for cases where the signals have a continuous decay in the pseudo-dimension, so that the corresponding Fourier transform is a compact pseudo-lineshape at zero frequency. The 3D method also requires that the pseudo-dimension has enough points for a meaningful Fourier transform. In our first  $T_2$  dataset, we collected planes at ten  $\tau$  values total, with duplicate measurements for three of these. The duplicate  $\tau$  values add discontinuities to the apparent evolution of signals in the pseudo-dimension. Such discontinuities give rise to truncation wiggles in the corresponding pseudo-spectrum, making them less sparse, and therefore less amenable to NUS reconstruction.

To explore this point, we used the second fully sampled  $T_2$  dataset (12 non-repeating  $\tau$  values with the last four planes out of  $\tau$  order) to produce a 25% and 50% uniform-randomly sampled NUS data (Representative Sampling Schedules; Fig. S3). The resampled data was processed using the 3D

pseudo-NUS method with and without sorting the 12 planes, and the 25% sampled dataset was also processed plane-wise using the traditional 2D IST method. SPARKY was used to extract signal evolutions from the resulting spectra and fit them to exponential functions (Eq. 1) using non-linear least squares analysis to extract the characteristic decay time  $\alpha$ . (Goddard and Kneller 2008; Lee et al. 2015). Errors in  $\alpha$  values were estimated by 15 Monte Carlo error analysis trials, each with similar variance as the original fit. Figure 2 shows  $T_2$  values from fully sampled data compared to values from 2D IST and 3D pseudo-NUS reconstructions, with results summarized in Tab. ST1. These results show that the 3D pseudo-NUS method can enable sampling at 25% density, where 2D reconstruction does not. From these examples, it is also clear that sorting the planes in  $\tau$  order gives best results. However, at 50% sampling, the improvements are minimal, because 50% density is already sufficient for good 2D reconstruction.

To further test the compressibility of the data, we explored the effect of the number of planes on the reconstruction. The 25% randomly sampled dataset was truncated to remove the last planes, producing datasets with 8, 9, 10, and 11  $\tau$  values. Each of these truncated datasets was reconstructed using the 3D pseudo-NUS method with and without sorting the planes in  $\tau$  order, and  $T_2$  relaxation times were extracted as above. Comparison of  $T_2$  values for these cases are shown in Fig. 2, a comparison of evolving 1D traces from the spectra is shown in Fig. S3, and the correlation coefficients comparing intensities and  $\alpha$  values from fully sampled and NUS reconstructions are given in Tab. ST1. It can be seen that sorting the planes in  $\tau$  order has a greater role in improving the reconstruction than increasing the number of planes from 9 to 12. Having less than nine planes in the pseudo-3rd dimension, however, leads to a less accurate reconstruction of the relative intensities, affecting the  $\alpha$  value obtained from the fit.

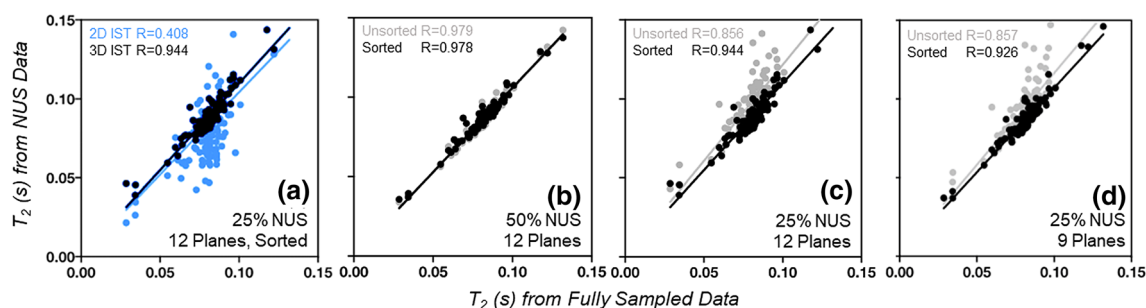


**Fig. 2** Correlation of  $T_2$  relaxation time estimated from fully sampled and uniform-random NUS spectra with 12 planes at non-repeating  $\tau$  values, labeled with Pearson's R correlation values. Comparisons for reconstructions using unsorted planes are in gray, and comparisons for reconstructions of planes sorted in  $\tau$  order are in black. **a** Correlation of  $T_2$  relaxation times calculated from the traditional 2D IST

Pseudo-NUS reconstructions of the  $T_2$  data showed good intensity correlation with fully sampled data, however some schemes systematically overestimate the  $\alpha$  value by about 10%, as can be seen in Fig. 2. This was also seen in similar reconstructions of the  $T_1$  data. To better identify the acquisition and processing schemes to eliminate the possibility of systematic error, we studied the effects of (1) the spacing of  $\tau$  values in the pseudo-dimension, (2) the maximum  $\tau$  value, and (3) the type of sampling schedule. Changing the spacing in the pseudo-dimension changes the total amount of signal captured in the 2D series, and importantly, it changes the pseudo-lineshape produced by Fourier transform of the pseudo-dimension. This can influence the effectiveness of NUS, since broad signals or signals with truncation artifacts can be considered as less sparse than sharp lines without artifacts. Therefore, to test whether a linear or exponentially increasing  $\tau$  delay produces more accurate reconstructions, we created simulated time-domain data mimicking the previously collected fully-sampled  $T_1$  data and its  $\alpha$  values, using either a linear spacing or exponential spacing between  $\tau$  values (Fig. 3).

To generate a more realistic simulation, each peak had small random perturbations to its  $^1\text{H}$  and  $^{15}\text{N}$  linewidths and phases, and random unresolved couplings (Nichols et al. 2020); example spectra and simulation details are given in Fig. S4. To test the effect of maximum  $\tau$  delay ( $\tau_{max}$ ), we created simulations with a  $\tau_{max}$  of 0.800 s, 1.600 s, or 3.200 s, using both linear and exponential  $\tau$  spacing, resulting in six fully sampled time-domain datasets.

To include the effects of sampling schedule type, this simulated data was resampled according to either uniform random or sine-weighted Poisson-gap schedules, for a total of 12 sparsely sampled datasets. Poisson-gap schedules were created using the istHMS schedule generator utility (Hyberts et al. 2010; Hyberts et al. 2012).

method (blue) and the 3D pseudo-NUS using IST. **b** Correlation of  $T_2$  relaxation times calculated from 50% sampled data. **c** Correlation of  $T_2$  relaxation times calculated from 25% sampled data. **d** Correlation of  $T_2$  relaxation times calculated from 25% sampled data using only nine planes instead of 12

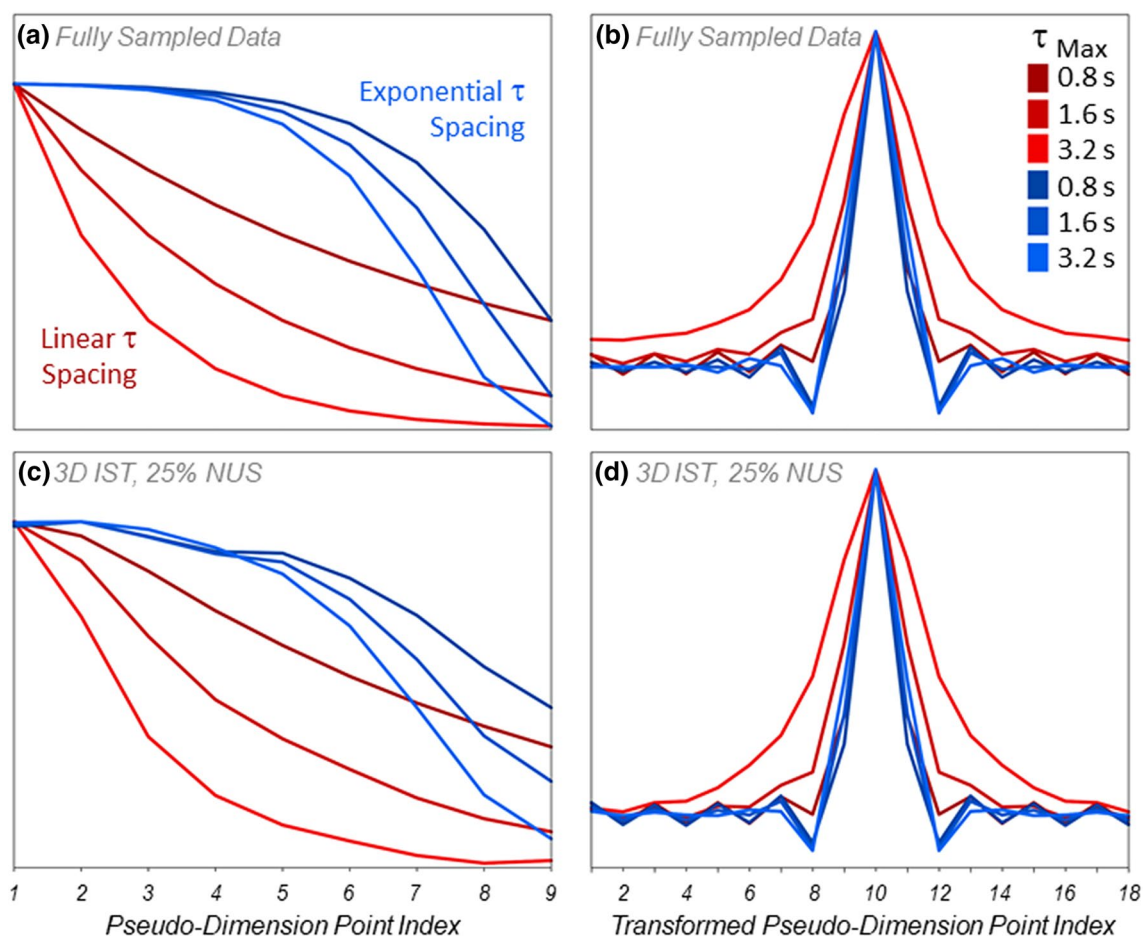


**Fig. 3** Effects of  $\tau$  spacing on evolutions of a selected peak. Results for exponential spacing are in blue, linear spacing in red. Panels **a** and **c** show the evolution curves from the reconstructed results, while panels **b** and **d** show the corresponding pseudo-spectra. Linear  $\tau$  spacing gives rise to an exponentially decaying profile, while measure-

ments with exponential  $\tau$  spacing give Gaussian evolutions when the pseudo-dimension is viewed as uniformly spaced points, corresponding to narrower pseudo-lineshapes that are more amenable to NUS reconstruction

The six fully sampled datasets were processed using traditional Fourier transform methods, the 12 sparsely sampled datasets were processed using the new 3D pseudo-NUS protocol, and  $\alpha$  values were extracted as above via SPARKY. The errors for each  $\alpha$  value were calculated across all 18 datasets, and the average and standard deviation of the errors for each dataset were determined (Tab. ST2). From these simulations, the best results were obtained from spectra sorted in  $t$  order, using Poisson-gap schedules, and with exponentially spaced  $\tau$  values to a  $\tau_{max}$  of about 2 times the  $1/\alpha$  value (here, 1.600 s). These best-case scenarios were also evaluated using hmsIST or SMILE for reconstruction as an alternative to NMRPipe's implementation of IST, with all methods producing comparably good results (Tab. ST1, Tab. ST3, Fig. S3, Fig. S5). As shown in Tab. ST2, all Poisson-gap examples with exponentially spaced  $\tau$  values produced percent errors of 0.5% or less, while other random uniform sampling

or linear  $\tau$  schemes had percent errors in the range of 4.0–15.6%.

In conclusion, we have shown that 3D pseudo-NUS is able to accurately reconstruct the intensities of non-uniformly sampled NMR data for  $T_1$  and  $T_2$  datasets and can do so with fewer NUS samples than if separate 2D reconstructions are used. Using real and simulated NUS data sampled at 25% density, we showed that for accurate reconstruction, six criteria in data collection and processing are important. These criteria are not surprising, because they make the pseudo-3D measurement behave most like data that gives sharp clean lines in all three dimensions when subjected to complete 3D reconstruction: (1) the planes must be reordered to have an increasing  $\tau$  delay in the pseudo-dimension prior to processing, (2) the planes should not include repeating  $\tau$  values, (3) the  $\tau$  values should be exponentially increasing in the pseudo-3D dimension, (4) Poisson-gap schedules give a substantial improvement, (5) 9 to 12 planes give the

best results, and (6) the most accurate fits occur when the maximum  $\tau$  value is approximately twice the characteristic exponential decay time.

Using 3D pseudo-NUS and these criteria, we were able to reduce collection time of  $T_1$  and  $T_2$  data by a factor of four and obtain accurate  $T_1$  and  $T_2$  decay rates. This method can be combined with other time-saving techniques to further reduce the experimental burden for obtaining relaxation parameters. The new method has the additional advantage that it is based upon existing reconstruction methods that have already been well-characterized for 3D applications, this relaxation application being a special case. Spectral data and processing scripts are available for download, and the NMR software programs used are available on NMRBox (Maciejewski et al. 2017).

**Supplementary Information** The online version contains supplementary material available at <https://doi.org/10.1007/s10858-021-00369-7>.

**Acknowledgements** This work was supported by start-up funds from Brown University and funds from the COBRE Center for Computational Biology of Human Disease (NIH P20-GM109035).

**Disclaimer** Certain commercial equipment, instruments, and materials are identified in this presentation in order to specify the experimental procedure. Such identification does not imply recommendation or endorsement by the National Institute of Standards and Technology, nor does it imply that the material or equipment identified is necessarily the best available for the purpose.

**Data availability** Example processing and analysis scripts and data will be available via the NMRPipe web site: <https://www.ibbr.umd.edu/nmrpipe>.

**Software availability** The work makes use of the following software, which is all also available on the NMRbox cloud computing platform: NMRbox: <https://www.nmrbox.org>, NMRPipe: <https://www.ibbr.umd.edu/nmrpipe/install.html>, SMILE: <https://spin.niddk.nih.gov/bax/software/smile>, hmsIST: <http://gwagner.med.harvard.edu/intranet/hmsIST> (download by request).

## Declarations

**Conflict of interest** Authors have no conflicting or competing interests to declare.

## References

- Amaral M, Kokh DB, Bomke J, Wegener A, Buchstaller HP, Eggenweiler HM, Matias P, Sirrenberg C, Wade RC, Frech M (2017) Protein conformational flexibility modulates kinetics and thermodynamics of drug binding. *Nat Commun* 8(1):2276
- Barna JCJ, Laue ED, Mayger MR, Skilling J, Worrall SJP (1987) Exponential sampling, an alternative method for sampling in two-dimensional Nmr experiments. *J Magn Reson* 73(1):69–77
- Baselice F, Ferraioli G, Grassia A, Pascazio V (2014) Optimal configuration for relaxation times estimation in complex spin echo imaging. *Sensors (basel)* 14(2):2182–2198
- Bostock M, Nietlispach D (2017) Compressed sensing: reconstruction of non-uniformly sampled multidimensional NMR data. *Concepts Magn Reson Part A* 46a(2):e21438
- Bostock MJ, Holland DJ, Nietlispach D (2012) Compressed sensing reconstruction of undersampled 3D NOESY spectra: application to large membrane proteins. *J Biomol NMR* 54(1):15–32
- Delaglio F, Grzesiek S, Vuister GW, Zhu G, Pfeifer J, Bax A (1995) NMRPipe: a multidimensional spectral processing system based on UNIX pipes. *J Biomol NMR* 6(3):277–293
- East KW, Newton JC, Morzan UN, Narkhede YB, Acharya A, Skeens E, Jogl G, Batista VS, Palermo G, Lisi GP (2020) Allosteric motions of the CRISPR-Cas9 HNH nuclease probed by NMR and molecular dynamics. *J Am Chem Soc* 142(3):1348–1358
- Goddard TD, Kneller DG (2008) SPARKY 3. University of California, San Francisco
- Hansen DF (2019) Using deep neural networks to reconstruct non-uniformly sampled NMR spectra. *J Biomol NMR* 73(10–11):577–585
- Hoch JC, Maciejewski MW, Filipovic B (2008) Randomization improves sparse sampling in multidimensional NMR. *J Magn Reson* 193(2):317–320
- Hyberts SG, Arthanari H, Robson SA, Wagner G (2014) Perspectives in magnetic resonance: NMR in the post-FFT era. *J Magn Reson* 241:60–73
- Hyberts SG, Milbradt AG, Wagner AB, Arthanari H, Wagner G (2012) Application of iterative soft thresholding for fast reconstruction of NMR data non-uniformly sampled with multidimensional Poisson gap scheduling. *J Biomol NMR* 52(4):315–327
- Hyberts SG, Takeuchi K, Wagner G (2010) Poisson-gap sampling and forward maximum entropy reconstruction for enhancing the resolution and sensitivity of protein NMR data. *J Am Chem Soc* 132(7):2145–2147
- Kazimierczuk K, Orekhov VY (2011) Accelerated NMR spectroscopy by using compressed sensing. *Angew Chem Int Ed Engl* 50(24):5556–5559
- Kleckner IR, Foster MP (2011) An introduction to NMR-based approaches for measuring protein dynamics. *Biochim Biophys Acta* 1814(8):942–968
- Lee W, Tonelli M, Markley JL (2015) NMRFAM-SPARKY: enhanced software for biomolecular NMR spectroscopy. *Bioinformatics* 31(8):1325–1327
- Linnet TE, Teilmann K (2016) Non-uniform sampling of NMR relaxation data. *J Biomol NMR* 64(2):165–173
- Lisi GP, Loria JP (2016) Using NMR spectroscopy to elucidate the role of molecular motions in enzyme function. *Prog Nucl Magn Reson Spectrosc* 92–93:1–17
- Loria JP, Rance M, Palmer AG (1999) A relaxation-compensated Carr-Purcell-Meiboom-Gill sequence for characterizing chemical exchange by NMR spectroscopy. *J Am Chem Soc* 121:2331
- Maciejewski MW, Schuyler AD, Gryk MR, Moraru PR II, Romero EL, Ulrich HR, Eghbalnia M, Livny FD, Hoch JC (2017) NMRbox: a resource for biomolecular NMR computation. *Biophys J* 112(8):1529–1534
- Maria-Solano MA, Serrano-Hervas E, Romero-Rivera A, Iglesias-Fernandez J, Osuna S (2018) Role of conformational dynamics in the evolution of novel enzyme function. *Chem Commun* 54(50):6622–6634
- Mobli M, Hoch JC (2014) Nonuniform sampling and non-Fourier signal processing methods in multidimensional NMR. *Prog Nucl Magn Reson Spectrosc* 83:21–41
- Monajemi H, Donoho DL (2019) Sparsity/undersampling tradeoffs in anisotropic undersampling, with applications in MR imaging/spectroscopy. *Inf Inference A J IMA* 8:531–576

- Nichols PJ, Born A, Henen MA, Strotz D, Jones DN, Delaglio F, Vogeli B (2020) Reducing the measurement time of exact NOEs by non-uniform sampling. *J Biomol NMR* 74(12):717–739
- Orekhov VY, Jaravine VA (2011) Analysis of non-uniformly sampled spectra with multi-dimensional decomposition. *Prog Nucl Magn Reson Spectrosc* 59(3):271–292
- Palmer AG 3rd (2004) NMR characterization of the dynamics of biomacromolecules. *Chem Rev* 104(8):3623–3640
- Qu X, Mayzel M, Cai JF, Chen Z, Orekhov V (2015) Accelerated NMR spectroscopy with low-rank reconstruction. *Angew Chem Int Ed Engl* 54(3):852–854
- Robson S, Arthanari H, Hyberts SG, Wagner G (2019) Nonuniform sampling for NMR spectroscopy. *Methods Enzymol* 614:263–291
- Schmieder P, Stern AS, Wagner G, Hoch JC (1994) Improved resolution in triple-resonance spectra by nonlinear sampling in the constant-time domain. *J Biomol NMR* 4(4):483–490
- Schmieder P, Stern AS, Wagner G, Hoch JC (1997) Quantification of maximum-entropy spectrum reconstructions. *J Magn Reson* 125(2):332–339
- Schuyler AD, Maciejewski MW, Stern AS, Hoch JC (2015) Nonuniform sampling of hypercomplex multidimensional NMR experiments: dimensionality, quadrature phase and randomization. *J Magn Reson* 254:121–130
- Stern AS, Donoho DL, Hoch JC (2007) NMR data processing using iterative thresholding and minimum  $l(1)$ -norm reconstruction. *J Magn Reson* 188(2):295–300
- Urbanczyk M, Nowakowski M, Kozminski W, Kazimierczuk K (2017) Joint non-uniform sampling of all incremented time delays for quicker acquisition in protein relaxation studies. *J Biomol NMR* 68(2):155–161
- Worley B, Powers R (2015) Deterministic multidimensional nonuniform gap sampling. *J Magn Reson* 261:19–26
- Ying J, Delaglio F, Torchia DA, Bax A (2017) Sparse multidimensional iterative lineshape-enhanced (SMILE) reconstruction of both non-uniformly sampled and conventional NMR data. *J Biomol NMR* 68(2):101–118

**Publisher's Note** Springer Nature remains neutral with regard to jurisdictional claims in published maps and institutional affiliations.